On identification and analysis of fundamental issues in Terfenol-D transducer modeling

Marcelo J. Dapino[*], *Frederick T. Calkins*,[†] *and Alison B. Flatau*[‡]
[*‡]AEEM Department, Iowa State University, Ames, IA 50011
[†] Boeing Co., M.S. 82-24, P.O. Box 3999, Seattle, WA 98124

ABSTRACT

Complete models of highly-magnetostrictive Terfenol-D transducers must be able to characterize the magnetostriction upon knowledge of the impressed electrical energy. Fundamental characterization laws are not available at present, because the existing modeling techniques fail to simultaneously span all operating regimes: electric, magnetic, mechanical, and thermal, across the whole performance space of these transducers. This paper attempts to capture the essential aspects of these regimes and their interactions, i.e. those that the transducer designer is likely to encounter during design, analysis and modeling of magnetostrictive devices. The issues discussed here are the magnetization and stress states, thermal effects, magnetomechanical hysteresis, AC losses, system nonlinearities, and transducer dynamics. In addition, some of the more relevant modeling techniques that address these issues are presented and analyzed.

Keywords: magnetostriction, Terfenol-D, transducer, modeling

1. INTRODUCTION

Magnetostriction is the change in shape exhibited by some materials when subjected to changes in the magnetization state. The phenomenon was first published by James Joule in 1842. Early work by the NDRC [1] and Bozorth [2], among others, surveyed the potential of the then available magnetostrictive materials (iron, nickel, cobalt, Permalloy) and provided insight on performance issues. Notably, by virtue of the reciprocity of the magnetostrictive effect, magnetostrictive transducers are capable of providing both actuation and sensing. The emergence of piezoelectric ceramics with approximately twice the coupling coefficient of nickel hindered the evolution of magnetostrictive materials for a long period of time. However, the interest in magnetostrictive materials for use in transducer applications has increased significantly during the past two decades. This is largely due to the development of more capable magnetostrictive materials, such as the rare-earth iron alloys Terfenol-D ($Tb_xDy_{1-x}Fe_y$, $0.27 < x < 0.3, 1.9 < y < 2$). These alloys are highly attractive in the transducer applications arena due to their room temperature strain and force capabilities [40].

Unfortunately, the increased use of magnetostrictive materials has not been accompanied by the availability of more complete and accurate transducer models. Complete models must incorporate the different operating regimes present in magnetostrictive transducers, in a manner compatible with the requirements of specific applications. The regimes present in magnetostrictive transducers are: electric (which links the transducer with the power supply amplifier through the excitation solenoid); magnetic (which involves routing of magnetic field through magnetic circuit for magnetization of the magnetostrictive core); mechanical (elastic state of the materials present in the transducer); and thermal (the temperature distribution in the transducer materials). Extensive experimental evidence [3, 4] demonstrates that it is crucial to consider the interaction between these regimes, therefore models for the various regimes need to be coupled to provide a complete description of a transducer system.

Most of the currently available models of magnetostrictive transducers fail to incorporate all regimes simultaneously. This is in part because transducer models are still predominantly based on the linear constitutive piezomagnetic

[*](Correspondence)- Email: marcelod@iastate.edu; Telephone: 515-294-0088; Fax: 515-294-8584
[†]Email: Frederick.Calkins@PSS.Boeing.com; Telephone: 253-773-4412
[‡]Email: abf@iastate.edu; Telephone: 515-294-0094

Part of the SPIE Conference on Smart Structures and Integrated Systems • San Diego, California • March 1998
SPIE Vol. 3329 • 0277-786X/98/$10.00

equations [5]. These equations neglect the effects of coupling between stress, magnetization, and temperature in the material, which have bearing on the mechanical performance as indicated by [6], among others.

Carman and Mitrovic [7], and Kannan and Dasgupta [8], extended the scope of the linear constitutive equations by including specific nonlinear effects. The nonlinear dynamics of magnetostrictive transducers has been also modeled following a phenomenological approach. One such approach is obtained through the use of generalized Preisach operators. Preisach models that specifically target giant magnetostrictive materials are discussed by Restorff et al. [9], Adly and Mayergoyz [10], and Smith [11]. These models provide characterization of different operating regimes, but are cumbersome to implement in magnetostrictive transducers where performance changes significantly during operation.

Other modeling efforts have combined physical laws with phenomenological observation. Engdahl and Berqvist [12] present a model capable of dealing with nonlinearities and various losses, such as magnetomechanical hysteresis, eddy currents, ohmic heating, and mechanical losses. Physically-based Preisach models combine the empirical robustness of non-physical laws with some understanding of the physical processes that govern magnetic and magnetostrictive hysteresis. Basso and Bertotti, for instance, develop in [13] a Preisach-based hysteresis model for materials where the magnetization is dominated by domain wall motion.

Nevertheless, there does not exist a fundamental model applicable to the complete performance space of magnetostrictive transducers. The development of physics-based models which incorporate the different operating regimes and the issues inherent to them will certainly extend the utility of these transducers. The purpose of this paper is to identify and analyze the most fundamental issues in magnetostrictive transducer modeling, and to review some of the current state-of-the-art modeling techniques which handle these issues.

2. DISCUSSION

Much of the performance of magnetostrictive materials such as Terfenol-D can be described by considering the combined effects of magnetization and stress. Under dynamic conditions additional effects play an important role in the transducer performance. These effects include thermal issues, magnetomechanical hysteresis, AC losses, system nonlinearities, and transducer dynamics. Most of these effects are coupled. For instance, eddy current power losses increase with approximately the square of frequency. Temperature and magnetization are also intrinsically coupled; it is well known in ferromagnetic materials that above the Curie temperature the long range coupling between magnetic moments is lost, due to thermal energy overcoming the interaction energy (energy that holds magnetic moments aligned within domains).

Material properties are directly related to those effects as well. In fact material properties are often used to gauge those effects and their interactions. Because of the intimate relationship between material properties and transducer performance, material properties are used to quantify, analyze, and model performance. Typical magnetic, elastic and magnetoelastic properties include: Young's modulus, mechanical quality factor, permeability, saturation magnetization and magnetostriction, axial strain coefficient, and magnetomechanical coupling coefficient. It is important to note that material properties and transducer performance are strongly coupled, so changes in operating parameters affect material properties and vice versa. This fact was studied in [14], where variations in material properties were measured under carefully controlled, varied transducer operating conditions (and hence under carefully controlled, varied transducer behavior). Prior work by Hall [3] had suggested material property variability; later work in [14] demonstrated material properties do vary with operating conditions, but they remain unchanged (within $\approx$ 5%) when operating conditions are fixed.

The above mentioned issues have both design and modeling implications. In fact compromises between design and modeling are sometimes present in particular transducer applications. For instance, designs that use laminated magnetostrictive cores and slit permanent magnets help minimize eddy current losses. For such designs simplified eddy current models or even models that neglect eddy current effects altogether may be appropriate. On the other hand, a poorly designed magnetic circuit may demand incorporation of eddy current effects in the mathematical models of the transducer for accurate prediction of transducer performance. Similar compromises between design and modeling are observed in other issues as well. For instance, thermal effects may be minimized by incorporating cooling devices in the transducer design which may subsequently help to simplify the modeling.

2.1 Magnetization

The magnetostrictive core is magnetized by the processes of domain wall motion and domain magnetization rotation. Depending on the net thermodynamic balance after application of an external field, these processes can

be either reversible (conservative) or irreversible (dissipative). Reversible phenomena occur only for small field increments and hence small magnetization changes.

In an attempt to minimize the total magnetostatic energy of the material, the magnetization breaks up in localized regions called magnetic domains, where magnetic moments associated with atoms in the material are aligned parallel. The boundary which separates neighboring domains is known as a domain wall. Domain walls constitute transition layers through which magnetic moments undergo reorientation and where there exists a delicate balance between interaction and anisotropy energies. The application of a magnetic field breaks this delicate energy balance and leads to domain wall motion and magnetization rotation.

Domain wall motion occurs as a consequence of the growth of domains whose magnetization is aligned favorably with respect to the applied field, at the expense of domains with magnetization opposing the field. This occurs primarily at low field levels. At moderate field strengths, the magnetic moments within unfavorably oriented domains overcome the anisotropy energy and suddenly rotate from the original position into one of the crystallographic "easy" axes closer to the field direction. This phenomenon is sometimes known as the "jumping" or burst effect, and the field that causes it is called the critical field. At moderate to high field strengths, the magnetic moments align themselves along crystallographic "easy" axes lying close to the field direction. As the field is increased further, the magnetic moments undergo coherent rotation until they reach alignment with the applied field resulting in single-domain material. This state is called technical saturation. Beyond this point, the increase in applied magnetic field produces the so called state of forced magnetization, which in turn leads to a state of forced magnetostriction. Extensive treatment of domain processes can be found in references [15, 16].

Operation around the critical field permits high output strains per unit applied field by taking advantage of the burst effect, and highlights the need for applying a magnetic bias to the transducer. The magnetic bias is supplied by DC currents circulating through the excitation coil and/or permanent magnets. The selection of either method highly depends upon compromises between ohmic heating, power requirements, and allowable weight. Another issue that presents high interest for transducer applications is the change in Young's modulus with magnetic bias, known as the ΔE effect, which can be used to shift the mechanical resonance of the system [27]. This effect is used for tuning a Terfenol-D vibration absorber transducer in [29].

The effect of AC magnetic fields on dynamic transducer performance has been documented in [14, 17]. Figure 1(a) shows the effect of AC magnetic fields on the transducer's electrical impedance ($Z_{ee} = \frac{V}{I}$). The blocked electrical impedance, represented by the overall slope of $mag(Z_{ee})$, increases with applied field. The peak and valley of $mag(Z_{ee})$, which contain information on the transduction of energy between mechanical and electrical sides, shift differentially towards lower frequencies as the AC field strength is increased, indicating increased transduction.

The magnetization processes, and the magnetoelastic interactions in general, taking place inside the magnetostric-

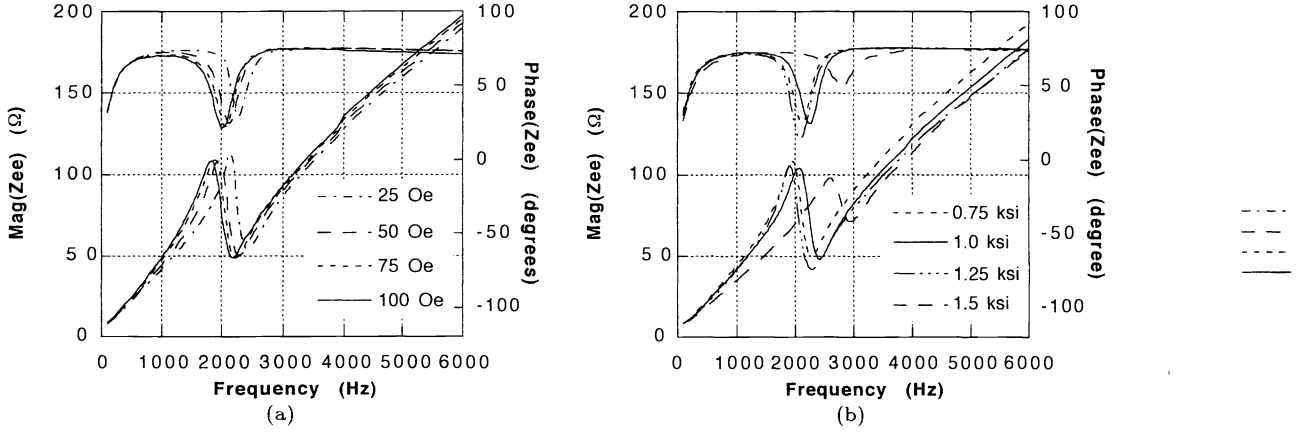

Figure 1: Total electrical impedance versus frequency, $mag(Z_{ee})$ Ω, and $phase(Z_{ee})$ degrees. (a) Bias condition 5.2 MPa, 24 kA/m (0.75 ksi, 300 Oe); AC fields: 2, 4, 6, 8 kA/m (25, 50, 75, 100 Oe); (b) Bias conditions: 5.2 MPa, 24 kA/m (0.75 ksi, 300 Oe); 6.9 MPa, 33.2 kA/m (1 ksi, 415 Oe); 8.6 MPa, 38.4 kA/m (1.25 ksi, 480 Oe); and 10.4 MPa, 43.2 kA/m (1.5 ksi, 540 Oe); AC field strength: 8 kA/m (100 Oe). From ref. [4].

tive core have been modeled in different manners. One such approach is to consider the material at its micromagnetics level. Classical micromagnetics work by Brown [18] assumes the material is simultaneously magnetizable and deformable with its energy state defined by elasticity, thermodynamics, and electromagnetic principles. Recent work in this field deals specifically with Terfenol-D [19]. Although the modeling results are useful at the domain level, the extension of micromagnetic models to describe the performance of Terfenol-D transducers in all regimes is a major task.

The Preisach model has been used extensively for characterization of ferromagnetic materials, and more recently of magnetostrictives as well. Much research effort has been devoted to accommodate physical aspects into the Preisach approach, which in its original form is unable to be traced back to fundamental principles. Reimers and Della Torre implement in [43] a fast inverse hysteresis model amenable to control applications, and with potential applicability to magnetostrictive materials.

Following the classical anisotropy domain rotation model by Stoner and Wohlfarth [41], Lee and Bishop [42] extended this idea to a random assembly of domain particles having cubic anisotropy. Clark et al. [25] included compressive loading along the [111] direction in a two dimensional scheme. Jiles and Thoelke [26] generalized this model to three dimensions, by considering the anisotropy, magnetoelastic, and field energies along all three directions. Although model results are in good agreement with measured data, the identification of the fractional occupancies which define the participation of different easy axes in the total magnetization is, by no means, trivial.

Another modeling approach which yields significant results is the ferromagnetic hysteresis model. Theory by Jiles and Atherton [20] predicts quasi-static $M - H$ loops in ferromagnetic materials by considering the energy of domain walls as they bow and translate during magnetization. Later extensions include models of magnetostriction, eddy current losses, minor loops, and mechanical prestress (see [21]). The appeal of the Jiles-Atherton model stems from the physical basis of the model parameters and the fact that only five parameters are needed for complete description of the magnetic state of the material. However, this model is purely magnetic in nature, which highlights the need for accurate and general magnetomechanical characterization laws to completely describe the transduction process in the transducer.

2.2 Stress

It is common practice to place a Terfenol-D sample under a mechanical compressive prestress for operation. The ability of the material to survive high accelerations and shock conditions improves under compressive stress since Terfenol-D is much more brittle in tension (tensile strength $\approx$ 28 MPa) than in compression (compressive strength $\approx$ 700 MPa) [22]. In addition, adequate preloading is capable of improving the magnetic state in the material as a consequence of the coupling between the magnetic and mechanical states. From the point of view of the energy balance in the material, the mechanical prestress is an additional source of anisotropy energy which in fact competes against the magnetocrystalline anisotropy, strain, and applied field energies. The application of a compressive preload forces a larger population of magnetization vectors to align perpendicular to the direction of application of the preload, where a state of local minimum energy is reached. This translates into both a smaller demagnetized length and increased saturation magnetostriction. However, for compressive preloads larger than a certain value, the prestress energy overpowers the elastic energy produced by the material and the magnetostriction decreases. In summary, the application of moderate preloads is motivated by mechanical (brittleness of Terfenol-D) and magnetomechanical (shift in overall energy balance inside the material and improved magnetostriction) reasons.

The effect of preload on overall performance is often illustrated with strain versus applied field curves, such as those of Fig. 2(a). These unbiased plots (sometimes known as "butterfly" curves) demonstrate the dependence of *transducer* output on prestress. For the prototype transducers studied (designed for operation under a 6.9 MPa nominal compressive prestress), peak strains are reached for prestresses of between 4.2-8.4 MPa, which is in remarkable contrast with results obtained with bare magnetostrictive cores statically loaded (i.e., subject to a dead weight) as discussed in [21]. The difference lies in the energy lost in the prestress mechanism (springs) within the transducer. These losses are not present in statically loaded samples which often exhibit peak performance at about 14 MPa and appreciable strains at prestresses of as high as 28 MPa [36]. Note the output from the dynamic transducer used in Fig. 2 is practically blocked at about 12 MPa. The losses in the prestress mechanism may be minimized by reducing the effective spring stiffness, although this presents the additional complication of shifting the transducer resonant frequencies.

Similar trends are observed in the M-H curves of Fig. 2(b), which show the dependence of the instantaneous susceptibility ($\frac{\partial M}{\partial H}$) on mechanical prestress [23, 4]. As the preload is increased, the value of the instantaneous susceptibility averaged over the burst region decreases.

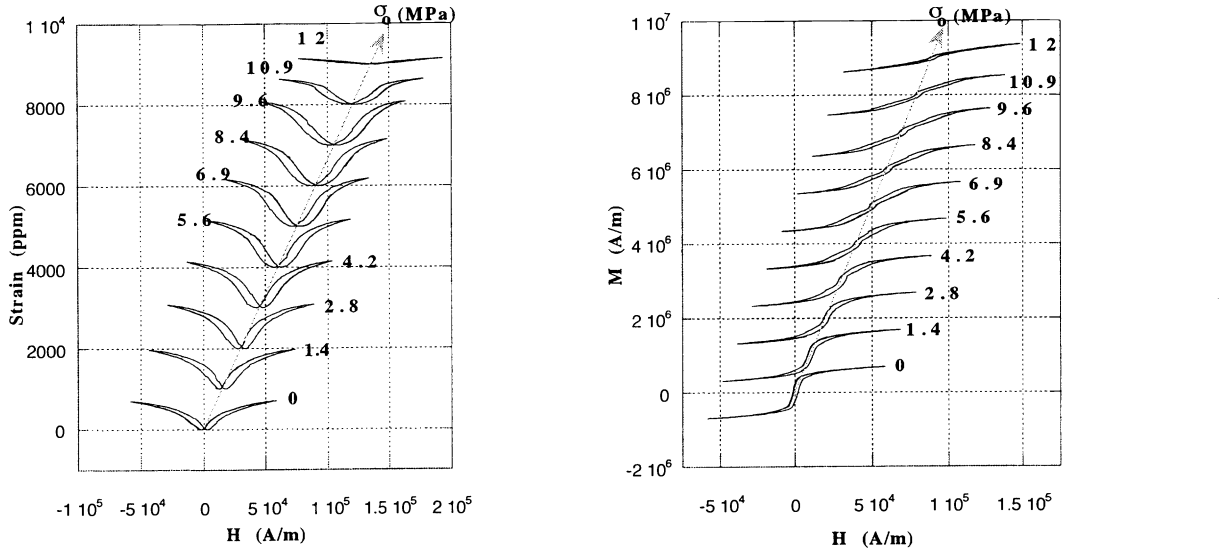

Figure 2: (a) Magnetostriction, and (b) magnetization, versus applied field, for 0, 1.4, 2.8, 4.2, 5.6, 6.9, 8.4, 9.6 and 12 MPa. ISU transducer, 12.7 mm diameter solid material, near-DC frequency of operation.

The relationship λ-M has been reported to be nearly independent of prestress except for very low prestresses and high magnetizations. Clark et al. [36] report a range of about 15-55 MPa for the λ-M stress independence in Bridgman-grown samples. In addition, work by Kvarnsjö [37] indicates that at high prestresses the primary magnetization mechanism is domain magnetization rotation, and as a consequence the quadratic law for magnetostriction discussed in section 2.4.2 is appropriate. Consistently, Clark et al. [25] found the quadratic law is incorrect in the low prestress regime (below 30 MPa for statically loaded, single crystal material) where it was found that strain does depend directly on stress and the magnetostriction cannot be accounted for by a single-valued magnetization law, i.e. hysteresis is observed.

2.3 Coupling between magnetization and stress

The magnetization and stress states in the material are intrinsically coupled. This effect is sometimes known as the dual magnetostrictive effect. Application of a magnetic field generates strains and hence stresses in the material, and application of stresses generates changes in the magnetization state.

As mentioned in section 2.1, magnetic biasing can lead to improved performance and hence it offers potential for performance optimization. The effects of the magnetization bias in the material are readily appreciable and manifest as changes in efficiency, coupling, axial strain coefficient, permeability, and elastic modulus. Further control of transducer performance can be exerted by subjecting the Terfenol-D element to both a magnetic bias and a compressive preload [28]; this situation is known as a "bias condition". Figure 1(b) shows the effect of bias condition on transducer total electrical impedance. As both the prestress and magnetic bias increase the blocked impedance decreases, whereas the mobility resonance shifts towards higher frequencies.

In reference [4] the authors investigated the effect of three bias conditions at different drive levels by measuring quasi-static strain at the field strengths 4, 8, and 16 kA/m (50, 100, and 200 Oe), as illustrated in Fig. 3, top to bottom. From left to right in Fig. 3, the three bias conditions are: 5.2 MPa, 24 kA/m (0.75 ksi, 300 Oe); 6.9 MPa, 33.2 kA/m (1.0 ksi, 415 Oe); and 8.6 MPa, 38.4 kA/m (1.25 ksi, 480 Oe). At each bias condition the minor loop nominal slope increases with increasing applied field; at a given drive level across bias conditions, the minor loop nominal slope decreases with increasing prestress. These clear trends are not seen in Figure 2(a), where the nominal slope of the strain-applied field curve remains approximately unchanged with prestress over a wide range of prestresses. These results highlight the importance of analyzing both minor and full-stroke loops during performance optimization; the more commonly available full-stroke curves do not provide all the necessary information for complete performance analysis.

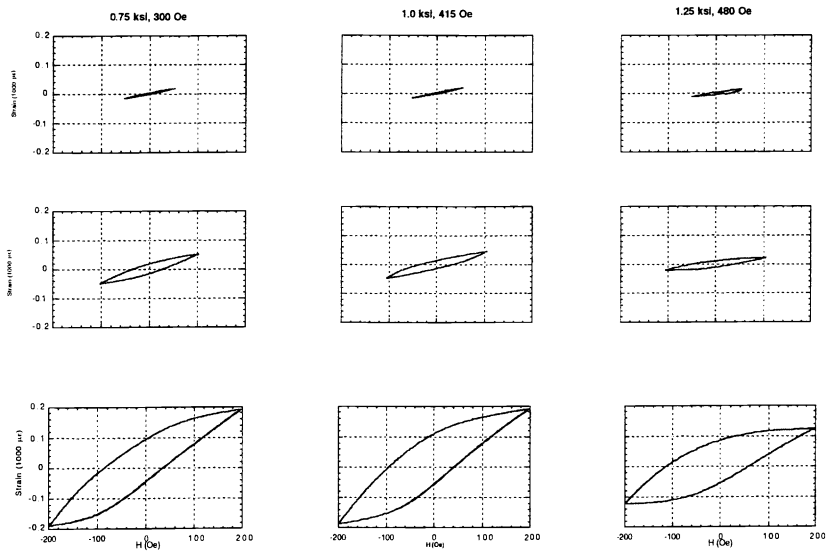

Figure 3: Strain-applied field minor loops. Bias conditions (left to right): 5.2 MPa, 24 kA/m (0.75 ksi, 300 Oe); 6.9 MPa, 33.2 kA/m (1.0 ksi, 415 Oe); and 8.6 MPa, 38.4 kA/m (1.25 ksi, 480 Oe). AC drive fields (top to bottom): 4, 8, 16 kA/m (50, 100, and 200 Oe). ISU 12.7 mm diameter rod transducer, 0.75 Hz excitation. From [4].

2.4 Additional operating effects

2.4.1 Thermal effects

It has been reported [6] that the performance of Terfenol-D is strongly affected by operating temperature. For instance, Figures 4 (a) and 4 (b) show magnetostriction and magnetic induction versus applied field under 13.3 MPa (1.93 ksi) prestress at -50, 0, 20 and 80 °C. The observed differences are significant. In particular, the magnitude of the magnetostriction at a field level of 159 kA/m (2000 Oe) increases nine-fold from -50 °C ($200 \times 10^{-}6$) to 0 °C ($1740 \times 10^{-}6$). This issue highlights the importance of operating the transducer near the optimal temperature regime (around room temperature for $Tb_{0.3}Dy_{0.7}Fe_{1.9}$).

In $Tb_{0.3}Dy_{0.7}Fe_{1.9}$ alloys, the maximum ratio magnetostriction/anisotropy (known as anisotropy compensation) occurs near room temperature. Large anisotropy compensations insure easy magnetization rotation and minimum hysteresis. As the temperature increases above the anisotropy compensation temperature different magnetization processes dominate, thus accounting for the changes in the material's performance. At temperatures well below the anisotropy compensation temperature (for instance, -50 °C), the less magnetostrictive <100> axes are magnetically easy. The primary magnetization mechanism is 180° domain wall motion, with some magnetization rotation from <100> to <111> axes, and hence the material is capable of very little magnetostriction. As temperature is increased from -50 °C to 0 °C, an applied field causes an order of magnitude increase in magnetostriction. This large increase in magnetostriction is due in part to the burst or "jumping" effect, which occurs when the magnetization rotates from one easy <111> axis to another <111> axis oriented closer to the applied field direction. Above the anisotropy compensation temperature, the highly magnetostrictive <111> axes are magnetically easy. As the temperature is increased further above room temperature, the magnetostriction decreases slightly, due to the reduction in the saturation magnetostriction with temperature above room temperature. At even higher temperatures, further changes occur until the Curie temperature ($\approx 380 - 430$ °C) is reached, where Terfenol-D becomes paramagnetic and the magnetostriction drops to zero.

The temperature effect has been incorporated in the linear piezomagnetic model discussed in section 2.4.4. Furthermore, by considering higher order interactions between magnetization, stress, and temperature, Carman and Mitrovic [7] developed a model capable of producing results in good agreement with experimental data at high preloads. However, the model is not capable of predicting saturation effects. Following the lead of Hom and Shankar [30], Duenas, Hsu and Carman [5] developed an analogous set of constitutive equations for magnetostriction. These equations are given by

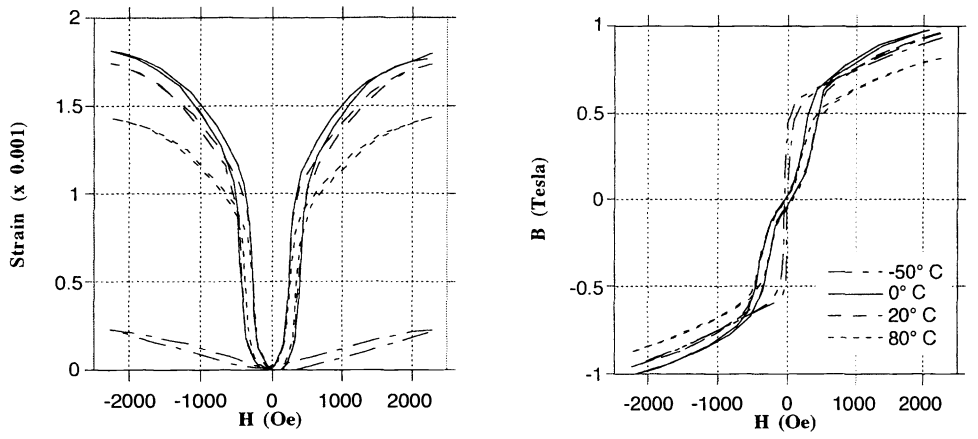

(a) (b)

Figure 4: Quasi-static temperature dependence; (a) magnetostriction, and (b) magnetic induction, versus applied field. (From [6], © 1992 Technomic Publishing Co., Inc.)

$$\varepsilon_{ij} = s^{M,T}_{ijkl}\,\sigma_{kl} + Q^{T}_{ijkl}\,M_k\,M_l + \alpha^{M}_{ij}\,\Delta T,$$
$$H_k = -2\,Q^{T}_{ijkl}\,M_l\,\sigma_{ij} + \frac{M_k}{k|M|}\,\mathrm{arctan}h\left(\frac{|M|}{M_s}\right) + P^{\sigma}_{k}\,\Delta T, \tag{1}$$

where ε is strain, s is compliance, Q is the magnetostrictive parameter, M and M_s are magnetization and saturation magnetization, α is coefficient of thermal expansion, T is temperature, H is magnetic field, P is the pyromagnetic coefficient, and k is a constant. Superscripts indicate the constant physical condition under which the parameter is measured, and subscripts indicate tensor order following conventional notation. This model successfully captures the quadratic nature of magnetostriction for low to medium field levels, but does not completely describe the saturation characteristics. The model allows incorporation of magnetostrictive hysteresis via complex model parameters.

Heat not only affects the magnetization processes in the magnetostrictive core, but it has bearing on the overall transducer design as well. Together with magnetomechanical hysteresis and eddy current losses, ohmic heating in the excitation coil is perhaps one of the most significant sources of losses. Other thermal effects to consider in transducer design are thermal expansion of the magnetostrictive core itself ($\alpha \approx 12 \times 10^{-6}/°\mathrm{C}$ [22]), dependence of material properties and performance of Terfenol-D on temperature, thermal expansion of the coil (coils used in prototype transducers showed expansion above 1.5% when heated to temperatures of around 100 °C), thermal expansion of other transducer components, and the thermal range of the coil insulation. Maintaining controlled temperatures during operation is critical for certain transducer applications. One clear example of this is precision machining. Transducers for this type of application need to use efficient thermal sinks, either active (cooling fluids), passive (thermally conducting materials, superconducting solenoids), or a combination of the two.

2.4.2 Magnetomechanical hysteresis

Magnetostrictive materials exhibit classical magnetic hysteresis. This phenomenon is evidenced in plots of magnetic induction (B) versus (H), which frequently have the familiar "sigmoid" shaped curve. One explanation of this phenomenon, first suggested by Wiedemann in 1886, is that a frictional type force is responsible for opposing the changes in magnetization. This hypothesis is consistent with the smooth changes in the magnetization seen on traversing the hysteresis loop as opposed to other theories which predict rapid switching of the magnetization yielding square loops [20]. Under frictional type force theories, hysteresis losses occur as a result of impedance to changes in the magnetization produced by imperfections in the material at locations known as pinning sites. Pinning sites are material imperfections such as crystal defects, grain boundaries, inhomogeneities within grains (dislocations and second phase materials), or regions of inhomogeneous stress. The amount of energy dissipated during domain wall pinning depends on the nature of the imperfection itself as well as on the relative direction of the magnetic moments on either side of the wall.

Another cause of hysteresis is the anisotropy of the crystal structure. The action of an applied field will cause a domain magnetization vector to jump from an initial orientation to a preferred orientation with lower energy. The irreversibility of this process also translates into energy loss.

Hysteresis is also seen in graphs of strain (λ) versus magnetization (M). The quadratic magnetostrictive law

$$\lambda = \frac{3}{2}\lambda_s \left(\frac{M}{M_s}\right)^2 \tag{2}$$

where λ_s is saturation magnetostriction and M_s is saturation magnetization, indicates strain is a single-valued function of the magnetization, thus anhysteretic. This anhysteretic law is not completely general, as evidenced by the λ-M plot in Figure 5, where a significant amount of hysteresis was measured under a 13.6 MPa preload. However, the quadratic law is used extensively to model magnetostriction under sufficient prestress, where domain magnetization rotation is thought to be the dominating magnetization process.

The hysteresis model for ferromagnetic materials discussed in section 2.1 [20] is perhaps one of the most polished physics-based schemes for characterization of hysteretic $M - H$ relationships. The model assumes reorientation of magnetic moments within domains follows the anhysteretic (hysteresis-free) magnetization predicted by the Langevin classical model for dilute paramagnetic materials. The hysteretic or total magnetization is then characterized by two components, $M_{tot} = M_{rev} + M_{irr}$. The reversible component of magnetization, M_{rev}, quantifies how much domain walls bulge before breaking free from pinning sites. The irreversible component, M_{irr}, quantifies the energy dissipation as domain walls translate and encounter pinning sites. The amount of hysteresis and the overall shape of the $M - H$ sigmoid are determined by means of physics-based parameters, which have been identified for specific materials under specific operating conditions [38].

2.4.3 AC losses

Dynamic operation leads to additional complications in the performance of Terfenol-D transducers. One important loss factor to consider is the eddy (or Foucault) currents. As modeled by the Faraday-Lenz law, eddy currents are set up in the transducer's conducting materials to resist changes of magnetic flux. These currents produce a magnetic flux that resists the externally applied magnetic field, and simultaneously cause a non-uniform distribution of current density often known as "skin effect".

Classical eddy current power loss formulations assume complete magnetic flux penetration and homogeneous permeability throughout the material. This assumption is valid only for small material thicknesses (e.g. laminae), and hence it is invalid in thick cylindrical transducer cores. The characteristic frequency above which the homogeneity of penetration of the magnetic flux is compromised, for cylindrical samples, is given by

$$f_c = \frac{2\rho}{\pi D^2 \mu^\varepsilon}, \tag{3}$$

where ρ is the resistivity of the material ($\rho \approx 0.6 \times 10^{-6}\Omega$ m for Terfenol-D [22]), D is rod diameter, and μ^ε is the clamped permeability. For a 6.35 mm (0.25 in) diameter rod the characteristic frequency is about 3 kHz. Laminations in the magnetostrictive core, low operating frequencies, and slit permanent magnets help to mitigate the effects of eddy currents.

A modeling approach based on energy considerations is shown by Jiles in [31]. This approach considers eddy currents as a perturbation to the quasi-static hysteresis. The simplicity of this model is however offset by the limitations imposed by its assumptions. Since uniform flux penetration is assumed, its applicability is limited to thinly laminated material or low operating frequencies.

Another classical approach to the eddy currents issue is the one presented by Bozorth [2] among others. In this model a so called eddy current factor χ is used to account for the reduced inductance caused by the oppositely induced magnetic field. The complex quantity $\chi = \chi_r + j\chi_i$ can be written, for cylindrical current-carrying conductors, in terms of Kelvin ber and bei functions, and is dependent upon frequency of operation, f, and the characteristic frequency, f_c, as follows

$$\chi_r = \frac{2}{\sqrt{p}}\left(\frac{\mathrm{ber}\sqrt{p}\ \mathrm{bei}'\sqrt{p} - \mathrm{bei}\sqrt{p}\ \mathrm{ber}'\sqrt{p}}{\mathrm{ber}^2\sqrt{p} + \mathrm{bei}^2\sqrt{p}}\right),$$
$$\chi_i = \frac{2}{\sqrt{p}}\left(\frac{\mathrm{ber}\sqrt{p}\ \mathrm{ber}'\sqrt{p} + \mathrm{bei}\sqrt{p}\ \mathrm{bei}'\sqrt{p}}{\mathrm{ber}^2\sqrt{p} + \mathrm{bei}^2\sqrt{p}}\right), \tag{4}$$

where $p = \frac{f}{f_c}$ is a dimensionless frequency parameter. An alternative, simpler presentation of the same formulation is shown by Butler and Lizza in [32].

2.4.4 System nonlinearities

Terfenol-D transducers are nonlinear in many senses. First of all, the magnetostrictive core itself is magnetized nonlinearly under application of applied fields. The different magnetization processes that lead to this phenomenon were discussed in Section 2.1. The process by which Terfenol-D strains with magnetization is nonlinear as well, as illustrated in Fig. 5. The overall input-output relationship in the transducer is, in consequence, nonlinear.

The nonlinear input-output relationship manifests itself in different ways. For instance, for zero magnetic bias operation a very nonlinear type of transduction results where the output motion of the transducer has twice the frequency of the impressed current. Even the magnetically biased transducer has a regime of nonlinear output, which translates into wave form distortion. The amount of distortion varies with the strength of both the AC and DC components of the applied field. Under application of a magnetic bias and AC fields with 0-pk amplitude not exceeding the DC bias value, frequency doubling is avoided; and for low magnetostriction ($< \frac{1}{3}\lambda_s$, [3]) the transducer output can be considered approximately linear. This case is often referred to as the "low signal linear magnetostriction" operation regime. This is the 1.1 kA/m (14 Oe) magnetic field case in Fig. 6, where a DC bias of 1.6 kA/m was used to center operation in the burst region for a 6.9 MPa (1 ksi) preload. The low signal situation has been treated extensively in the literature. The most common approach used to model this case is given by the linearized constitutive equations for piezomagnetic materials

$$\begin{aligned} \varepsilon &= s^H \sigma + d_{33} H, \\ B &= d_{33}^* \sigma + \mu^\sigma H, \end{aligned} \tag{5}$$

where ε, σ are strain and stress in the material; s^H is mechanical compliance at constant applied field; $d_{33} \approx d_{33}^*$ is axial strain coefficient; μ^σ is permeability at constant stress; B is magnetic induction; and H is magnetic field. The linear magnetostriction equations shown above are inaccurate for transducer applications where strokes are large and hence of nonlinear character. This situation is depicted in Fig. 6, most noticeably for the 7.3 kA/m (91 Oe) drive strength. As the magnetic field intensity is increased the strain output increasingly deviates from the sinusoidal shape of the magnetic field input.

One way to characterize transducer performance in the linear portion of strain regime is by experimental identification of the coefficients, i.e. by determination of the linear relationship between the coefficients s^H, d_{33}, d_{33}^* and μ^σ, and the operating parameters H and σ in equations (5). To determine these coefficients (or "material properties"), Hall [3] combined the linear magnetostriction equations with linear transduction equations and a mechanical spring-mass-dashpot model of the transducer. The linear transduction equations provide a "black box" model of the relationship between electrical and mechanical sides of the transducer through the transducer's total electrical impedance. These equations can be written as follows,

$$\begin{aligned} V &= Z_e I + T_{em} v, \\ 0 &= T_{me} I + z_m v, \end{aligned} \tag{6}$$

where V and I are voltage and current across transducer leads; v is velocity; T_{em}, T_{me} are mechanical-to-electrical and electrical-to-mechanical transduction coefficients; and z_m is mechanical impedance.

Researchers in the area of commercial finite element analysis have been able to develop characterization solvers for magnetostrictive materials, capable of structural and magnetic linear analysis [39, 34]. These solvers utilize the linearized piezomagnetic equations to couple the mechanical, magnetic, and thermal regimes. This approach is highly attractive for its relative simplicity once the material property parameters have been characterized.

The major disadvantage of this modeling technique is that the identification process itself tends to be very

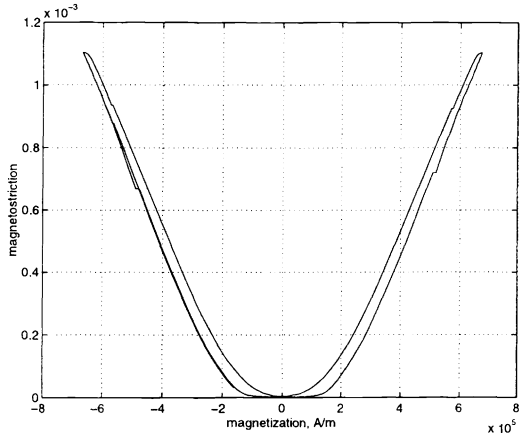

Figure 5: Magnetostriction versus magnetization for 12.7 mm (0.5 in) diameter by 11.5 mm (4.5 in) long, monolithic Terfenol-D under 13.6 MPa (1.95 ksi) preload.

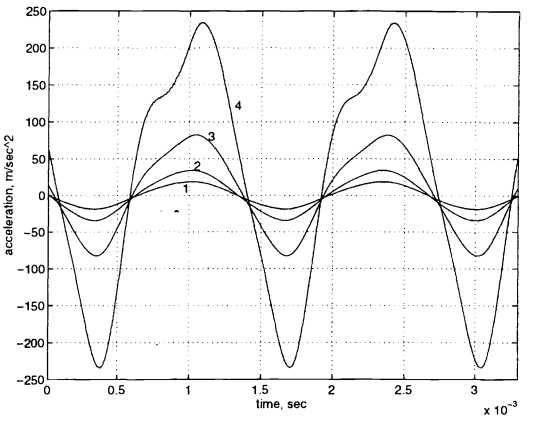

Figure 6: Acceleration versus time, at magnetic fields (1) 1.1 kA/m (14 Oe), (2) 3.7 kA/m (46 Oe), (3) 5.4 kA/m (67 Oe), and (4) 7.3 kA/m (91 Oe). Bias condition 6.9 MPa, 1.6 kA/m (1 ksi, 200 Oe).

laborious. The two year material property characterization study presented in [33, 14] yielded satisfactory results in the low signal operating regime. In that study over 80 different magnetostrictive rods were tested in 16 dynamic transducers to obtain material property information. This information was statistically analyzed and trends in material properties as a function of applied field, mass load, and temperature were identified. Two examples of these trends are shown in Fig. 7(a) and (b), where the open circuit elastic modulus, E_y^H, and the permeability at constant strain, μ^ε, are plotted against drive level for operation in four of the transducers. Further details on this research effort can be found in [17].

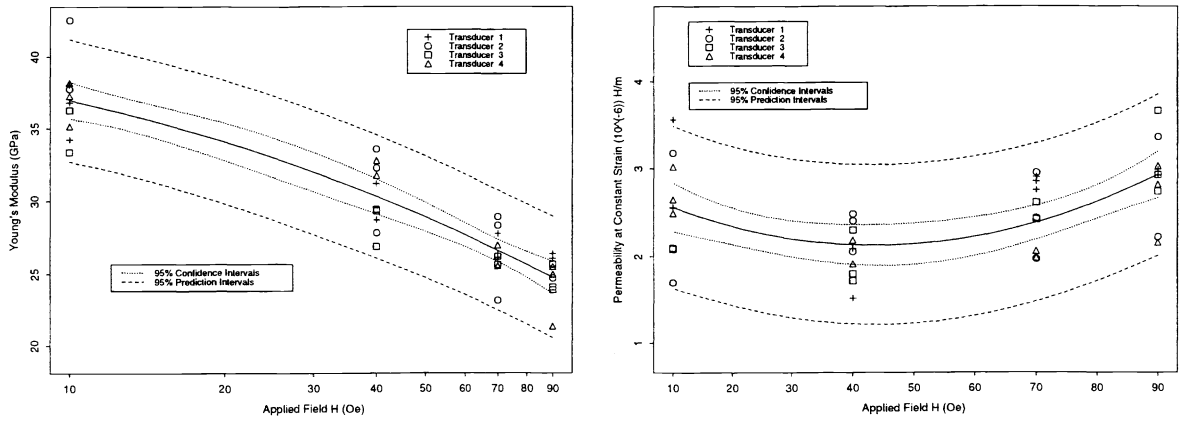

Figure 7: (a) Young's modulus at constant applied field, and (b) permeability at constant strain, versus applied field for ISU 12.7 mm (0.5 in) diameter transducers 1-4. Solid line is mean curve, dotted and dashed lines are 95% confidence and prediction intervals respectively.

Another source of potential nonlinearity in the transducer is the prestress mechanism. It is common design practice to place washers in magnetostrictive transducers, against which the magnetostrictive core is prestressed. As mentioned in section 2.2, this issue affects the performance of the magnetostrictive material when compared to material prestressed through application of a dead weight, because the washers act nonlinearly when compressed beyond a certain extent. In addition, they are a source of mechanical hysteresis and hence of losses which may prove to be fairly significant, as discussed in [21].

2.4.5 Transducer dynamics

As seen in Fig. 1 the resonant frequency of a Terfenol-D transducer varies significantly with operating conditions. The transducer mechanical resonance varies due to a number of factors. Some of these factors are the magnetostrictive core geometry, the bias condition (magnetic bias + mechanical prestress), AC magnetic field, external load, springs stiffness, and operating temperature. Other factors intrinsic to the specific design such as damping of internal components can be of significance as well.

The first mode mechanical resonance f_0 of a Terfenol-D transducer is given by

$$f_0 = \frac{1}{2\pi}\sqrt{\frac{k_{mc} + k_{ps}}{m_{eff}}}, \tag{7}$$

where k_{mc} is the magnetostrictive core stiffness, k_{ps} is the prestress mechanism stiffness, and m_{eff} is the system effective dynamic mass. The effective mass in the equation is formed by one-third of the mass of the rod plus the external load plus components of the prestress mechanism. Recognizing from theory of axial vibrations in slender cylinders that stiffness is inversely proportional to the material compliance, and since the compliance is strongly dependent upon operating conditions (Fig. 7(a)), the resonance frequencies of the magnetostrictive core will be strongly dependent on operating conditions. Increasing AC magnetic field intensity increases the system compliance hence decreasing transducer resonant frequencies (Figs. 1(a), 7(a)), while increasing prestress increases the system stiffness and hence resonant frequencies (Fig. 1(b)).

It was briefly mentioned in Section 2.3 that the shifts observed in the resonance frequency as the magnetic bias is changed can be used for tuning of an active vibration absorber. In fact, the capability to actively control the mechanical resonant frequency of the transducer is a powerful design tool which has been largely explored in the literature. This ability is not restricted to magnetostrictives, but is quite feasible in other transducer materials such as electrostrictives.

The dynamics of Terfenol-D transducers coupled to external loads are studied in [35]. An inplane force balancing model is used to consider both passive forces (those associated with the structural dynamics) and active forces (derived from the magnetostriction effect), to yield a PDE transducer model. The active component of the force is characterized through the strains predicted by the Jiles-Atherton ferromagnetic hysteresis model, combined with a magnetostriction quadratic law. The passive component is characterized through a PDE model of the transducer structural mechanics. The model is capable of predicting the quasi-static magnetization state of the transducer core, and of accurately predicting strains and displacements output by the transducer. The parameter requirements of this model are minimal, and the model is computationally non-demanding given the relative simplicity of the underlying PDE system. Work is in progress to incorporate the effects of AC losses.

3. CONCLUDING REMARKS

The high strains and forces achievable with Terfenol-D transducers has justified their use in a number of applications from sonar projectors to vibration control in heavy machinery. However, the relationship between input magnetic fields and output displacements has not been successfully characterized across the rich performance space offered by these transducers. The available models fail to span all the operating regimes simultaneously, let alone to characterize the complex interactions among those. An analytical approach was used by which the main issues that characterize each of the regimes and their interactions were identified. These issues, once identified and analyzed, will provide the transducer designer the necessary insight for efficient design of Terfenol-D transducers. This paper attempted to summarize these issues, as well as to address some of the available techniques for handling these issues and their interactions.

4. ACKNOWLEDGMENTS

The authors wish to acknowledge LeAnn Faidley and Brian Lund for their invaluable assistance in the data collection. Financial support for M.J.D. and A.B.F. was provided by the NSF Young Investigator Award #CMS9457288 of the Division of Civil and Mechanical Systems. The work of F.T.C. was funded by the NASA GSRP Award # 51254, Dr. Richard Silcox Program Manager.

References

[1] N.D.R.C., *The design and construction of magnetostriction transducers*, Office of scientific research and development, Summary Technical Report of Division 6, NDRC, Vol. 13, Washington, D.C., 1946.

[2] R. M. Bozorth, *Ferromagnetism*, D. Van Nostrand, Inc., New Jersey, 1968.

[3] D. Hall, "Dynamics and vibrations of magnetostrictive transducers," PhD dissertation, Iowa State University, Ames, IA, 1994.

[4] F. T. Calkins, M. J. Dapino, and A. B. Flatau, "Effect of prestress on the dynamic performance of a Terfenol-D transducer," *Proc. of SPIE Smart Structures and Materials*, Vol. 3041, pp. 293-304, San Diego, CA, March 1997.

[5] T. A. Duenas, L. Hsu, and G. P. Carman, "Magnetostrictive composite material systems analytical/experimental," *Adv. Smart Materials Fundamentals and Applications*, Boston, MA, 1996.

[6] A. E. Clark, "High power rare earth magnetostrictive materials," *Procs. Recent Advances in Adaptive and Sensory Materials and Their Applications*, pp. 387-397, Technomic Publishing Co., Inc., Lancaster, PA., 1992.

[7] G. P. Carman, and M. Mitrovic, "Nonlinear constitutive relations for magnetostrictive materials with applications to 1-D problems," *Journal of Intelligent Materials Systems and Structures*, V. 6, pp. 673-684, Sept. 1995.

[8] K. S. Kannan, and A. Dasgupta, "Continuum magnetoelastic properties of Terfenol-D; what is available and what is needed," *Adaptive Materials Symposium*, Summer Meeting of ASME-AMD-MD, UCLA, 1995.

[9] J. B. Restorff, H. T. Savage, A. E. Clark, and M. Wun-Fogle, "Preisach modeling of hysteresis in Terfenol-D," *J. Appl. Phys.*, **67**(9), pp. 5016-8, 1990.

[10] A. A. Adly, and I. D. Mayergoyz, "Magnetostriction simulation using anisotropic vector Preisach-type models," *IEEE Trans. Magn.*, **32**(5), pp. 4773-5, 1996.

[11] R. C. Smith, "Modeling techniques for magnetostrictive actuators," *Proceedings of SPIE Symposium on Smart Structures and Materials*, Vol. 3041, pp. 243-253, San Diego, CA, March 1997.

[12] G. Engdahl, and A. Berqvist, "Loss simulations in magnetostrictive actuators," *J. Appl. Phys.*, **79**(8), pp. 4689-91, 1997.

[13] V. Basso, and G. Bertotti, "Hysteresis models for the description of domain wall motion," *IEEE Trans. Magn.*, **32**(5), pp. 4210-12, 1996.

[14] M. Dapino, A. Flatau, and F. Calkins, "Statistical analysis of Terfenol-D material properties," *Proceedings of SPIE 1997 Symposium on Smart Structures and Materials*, Vol. 3041, pp. 256-267, San Diego, CA, March 1997.

[15] S. Chikazumi, *Physics of magnetism*, R. E. Krieger Publishing, Malabar, FL, 1984.

[16] B. D. Cullity, *Introduction to magnetic materials*, Addison-Wesley, Reading, Massachusetts, 1972.

[17] A. Flatau, J. Pascual, M. Dapino, and F. Calkins, "Material Characterization of ETREMA Terfenol-D- Final Report, Parts I- 0.25″ FSZM material, 12/96, and II- 0.5″ Bridgman material, 5/97," CATD-IPIRT #95-05.

[18] W. F. Brown, *Magnetoelastic interactions*, Springer-Verlag, Berlin, 1966.

[19] R. D. James, and D. Kinderlehrer, "Theory of magnetostriction with applications to $Tb_xDy_{1-x}Fe_2$," *Philosophical Magazine B*, **68**(2), pp. 237-74, 1993.

[20] D. C. Jiles, and D. L. Atherton, "Theory of ferromagnetic hysteresis," *J. Magn. Magn. Mater.*, **61**, p. 48, 1986.

[21] F. Calkins, "Design, analysis and modeling of giant magnetostrictive transducers," PhD dissertation, Iowa State University, Ames, IA, 1997.

[22] J. L. Butler, *Application manual for the design of ETREMA Terfenol-D magnetostrictive transducers*, ETREMA Products, Inc., Ames, IA, 1988.

[23] Trémolet de Lacheisserie, Etienne du, "Magnetostriction theory and applications of magnetoelasticity," CRC Press, Inc. Boca Raton, 1993.

[24] A. E. Clark, and J. P. Teter, "Magnetostriction 'jumps' in twinned $Tb_{0.3}Dy_{0.7}Fe_{1.9}$," *J. Appl. Phys.*, **63**(8), pp. 3910-12, 1988.

[25] A. E. Clark, H. T. Savage, and M. L. Spano, "Effect of stress on the magnetostriction and magnetization of single crystal $Tb_{0.27}Dy_{0.73}Fe_2$," *IEEE Trans. Magn.*, MAG-20, 5, September 1984.

[26] D. C. Jiles, and J. B. Thoelke, "Theoretical modelling of the effects of anisotropy and stress on the magnetization and magnetostriction of $Tb_{0.3}Dy_{0.7}Fe_2$," *J. Magn. Magn. Mater.*, **134**, pp. 143-160, 1994.

[27] A. E. Clark, J. B. Restorff, and M. Wun-Fogle, "Magnetoelastic coupling and ΔE effect in Tb_xDy_{1-x} single crystals." *J. Appl. Phys.*, **73** (10), 15 May 1993.

[28] M. B. Moffett, A. E. Clark, M. Wun-Fogle, J. Linberg, J. P. Teter, and E. A. McLaughlin, "Characterization of Terfenol-D for magnetostrictive transducers," *J. Acoust. Soc. Am.*, **89** (3), March 1991.

[29] A. B. Flatau, M. J. Dapino, C. S. Metschke, and F. Calkins, "High-bandwidth tunability in a smart passive vibration absorber," *Proc. of SPIE Smart Structures and Materials*, #3329-19, San Diego, CA, March 1998.

[30] C. L. Hom, and N. Shankar, "A fully coupled constitutive model for electrostrictive ceramic materials," *Second International Conference on Intelligent Materials*, ICIM, pp. 623-234, 1994.

[31] D. C. Jiles, "Frequency dependence of hysteresis curves in conducting magnetic materials," *J. Appl. Phys.*, **76** (10), pp. 5849-55, 1994.

[32] J. L. Butler, and N. L. Lizza, "Eddy current loss factor series for magnetostrictive rods," *J. Acoust. Soc. Am.*, **82**(1), July 1997.

[33] M. Dapino, A. Flatau, F. Calkins, and D. Hall, "Terfenol-D material properties under varied operating conditions," *Proceedings of SPIE Smart Structures and Materials*, #2717-66, San Diego, CA, March 1996.

[34] *ATILA, A 3D finite element code for piezoelectric and magnetostrictive transducers*, ISEN, Lille, France.

[35] M. Dapino, R. Smith, and A. Flatau, "An active and structural strain model for magnetostrictive transducers," *Proceedings of SPIE Smart Structures and Materials*, #3329-24, San Diego, CA, March 1998.

[36] A. E. Clark, J. P. Teter, M. Wun-Fogle, M. Moffett, and J. Lindberg, "Magnetomechanical coupling in Bridgman-grown $Tb_{0.3}Dy_{0.7}Fe_{1.9}$ at high drive levels," *J. Appl. Phys.*, **67**(9), 1 May 1990.

[37] L. Kvarnsjö, "On characterization, modeling and application of highly magnetostrictive materials," PhD dissertation, Royal Institute of technology, TRITA-EEA-9301, ISSN 1100-1593, Stockholm, Sweden, 1993.

[38] D. C. Jiles, J. B. Thoelke, and M. K. Devine, "Numerical determination of hysteresis parameters for the modeling of magnetic properties using the theory of ferromagnetic hysteresis," *IEEE Trans. Magn.*, Vol. 28, 1, January 1992.

[39] F. Claeyssen, R. Bossut, and D. Boucher, "Modeling and characterization of the magnetostrictive coupling," *Proc. Int. Workshop Power Transducers for Sonics and Ultrasonics*, Toulon, France, 1990.

[40] F. Claeyssen, N. Lhermet, R. Le Letty, "State of the art in magnetostrictive actuators," *Proc. 4th International Conference on New Actuators*, pp. 203-09 Bremen, Germany, June 1994.

[41] E. C. Stoner, and E. P. Wohlfarth, "A mechanism of magnetic hysteresis in heterogeneous alloys", *Phil. Trans. Roy. Soc.*, A240, pp. 599-642, 1948.

[42] E. W. Lee, and J. E. Bishop, "Magnetic behaviour of single-domain particles", *Proc. Phys. Soc.*, London, 89, p. 661, 1966.

[43] A. Reimers, and E. Della Torre, "Fast Preisach based magnetization model and fast inverse hysteresis model," IEEE, submitted.